



Glass transition evaluation of commercially available epoxy resins used for civil engineering applications



Julien Michels^{a,*}, Robert Widmann^a, Christoph Czaderski^a, Reza Allahvirdizadeh^b, Masoud Motavalli^{a,b}

^a Structural Engineering Research Laboratory, Swiss Federal Laboratories for Materials Science and Technology (Empa), Überlandstrasse 129, CH-8600 Dübendorf, Switzerland

^b School of Engineering, University of Tehran, Tehran, Iran

ARTICLE INFO

Article history:

Received 7 January 2015

Received in revised form

16 February 2015

Accepted 16 March 2015

Available online 25 March 2015

Keywords:

A. Thermosetting resins

B. Thermal properties

D. Thermal analysis

E. Cure

ABSTRACT

The paper presents a study about the glass transition of commercially available epoxy resins used for structural strengthening of concrete members for instance by means of Carbon Fiber Reinforced Polymer (CFRP) strips. Prior to an experimental investigation with a dynamic mechanical analysis (DMA), an overview on differences between definitions for the glass transition temperature T_g is given. Several testing recommendations are listed in this respect. Subsequently, DMA tests on three commercially available products are presented. A first focus is put on the different evaluation methods for one specific test result. It is visible that considerable differences in the finally adapted glass transition temperature might arise if one or the other procedure is followed. Additional parameters, such as curing procedure, specimen age, temperature history, and ultimate temperature during heating are considered, too. In all the above mentioned cases, differences in the glass transition can be found. Higher specimen age, higher ultimate temperature during testing, accelerated curing, as well as a lower heating rate implicate higher glass transition temperatures, showing that the glass transition temperature is not a fixed material characteristic. In a final step, the relevance for T_g for civil engineering applications is described. The various design code provisions for defining the service temperature in structures related to T_g are presented. The overall aim of the investigation is to show that structural engineers and end users have to be aware of the different influential parameters on the final results regarding the glass transition temperature, which also highlights the need of a potential deeper product investigation in case technical data sheets lack detailed information.

© 2015 Elsevier Ltd. All rights reserved.

1. Introduction

In civil engineering applications [4–6], epoxy resins are mostly used to bond a composite material, mainly Carbon Fiber Reinforced Polymer (CFRP) strips and sheets, to a concrete, metallic, or timber substrate. The two-component epoxy resins are usually mixed on site and require a certain curing time before being able to develop sufficient strength and stiffness [7]. The duration of this necessary curing time is generally depending on the product itself as well as on the outer temperature under which the cross-linking of the polymer chains has to take place. Fully or partly cured epoxy resins are prone to lose their stiffness and strength again when being

subjected to an increased temperature. For civil engineering applications, accidental situations like fire could lead to a deficient material and eventually serious structural safety problems. In general, high service temperatures influence the bond of a CFRP/epoxy/concrete system [8] and long-term creep behavior [9–13]. In order to describe a product's application range in terms of temperature stability, the producer or distributor declares a *glass transition temperature* denominated as T_g . In most of the cases, however, technical data sheets completely lack further information on which curing, testing, and subsequent evaluation parameters for the determination of T_g were followed. Whereas epoxy resins are usually cured under the ambient temperature, which should generally not be lower than 10°C due to a significantly decelerated curing process [7], it is known that an exposure to high temperatures in the range of 70–100°C can considerably reduce the necessary curing duration in order to achieve a target level of

* Corresponding author.

E-mail addresses: julien.michels@empa.ch, michels.julien@gmail.com (J. Michels).

Nomenclature

δ	shift angle
σ'	elastic stress
σ''	viscous stress
ϵ	strain amplitude
a	age
AC	accelerated curing
DMA	dynamic mechanic analysis
E'	storage modulus
E''	loss modulus
RT	room temperature curing
T	temperature
t	time
T_g	glass transition temperature
T_o	onset temperature at the tangent intersection
T_δ	temperature at maximum $\tan(\delta)$ value
T_{II}	temperature at maximum E'' value
T_i	temperature at the inflection point of E'
T_{max}	maximum temperature
T_{min}	minimum temperature
$\tan(\delta)$	ratio between loss and storage modulus

strength or stiffness [14–16]. This *accelerated curing* is for instance used for the application of a *gradient anchorage* for prestressed CFRP strips. In this procedure, the prestressing force is gradually decreased at both strip ends over several segments, interrupted by short localized accelerated adhesive curing steps [14,17,18]. The anchorage's mechanical response is in this case highly depending on the epoxy stiffness at a given temperature. To summarize, a degradation in stiffness (and possibly strength) of the resin due to elevated temperature can lead to a loss of anchorage capacity for a) initially unstressed strips but afterwards stressed under load during service, or b) for initially stressed strips in a gradient anchorage.

Glass transition is usually investigated by either *Differential Scanning Calorimetry* (DSC) or *Dynamic Mechanical Analysis* (DMA). It is important to notice that both DSC and DMA, since two different testing methods, usually provide slightly different results for identical curing conditions. For a DMA, a certain number of testing and evaluation parameters have to be considered. This paper presents in a first step a few internationally known testing recommendations and their respective suggestion on how to eventually evaluate the glass transition. In a second step, DMA tests and the results on three commercially available products often used in practice are presented. The main goal is to show influences of the curing conditions (room/ambient temperature and accelerated curing) with regard to the above mentioned gradient anchorage. Further material parameters, such as specimen age and heating rate during the DMA test are included in the analysis. Then, different methods for evaluating the glass transition and the effect of different test and curing parameters are discussed. In a final section, suggestions regarding temperatures at service level for strengthened civil structures by various structural design codes are presented. Finally, recommendations on how industry and design engineers shall proceed with glass transition and maximum service temperatures are given.

2. Glass transition and testing recommendations

2.1. General remarks

The expression *glass transition temperature* can be misleading, stating that exceeding a very precise temperature value leads to a

sudden change in material properties. This description has only limited applicability, since the transition from a solid to a rubber-like or viscous state is a continuous process over a certain temperature range of easily 10–20°C [19]. The previous indication of a temperature range is of qualitative nature, and should not be taken as absolute values for all adhesive types. A schematic representation of the elastic modulus decrease as a function of the temperature under laboratory testing condition is given in Fig. 1. It can be observed that the initial decrease of the elastic modulus occurs at a moderate rate, followed by a clearly higher rate between a certain *glass transition-range*. It has to be stated that the exact behavior under outer ambient conditions might differ due to different temperature scenarios.

2.2. Dynamic mechanical analysis (DMA) and definition of T_g

Dynamic Mechanical Analysis (DMA), which will be the experimental technique primarily applied and discussed in this manuscript, is used to assess the material property degradation under elevated temperature and cyclic loading. A resulting sinusoidal force is measured and correlated against the input strain. Then, the *viscous* and *elastic* properties of the sample are determined. If the sample behaves as an ideal elastic solid, then the resulting stress is proportional to the strain amplitude (ϵ , Hooke's Law), and the stress and strain signals are in phase. If on the contrary the sample behaves as an ideal fluid, stress is proportional to the strain rate ($d\epsilon/dt$, Newton's Law). In this case, the stress signal is out of phase with the strain, leading it by 90° (phase angle δ). For viscoelastic materials, the phase shift angle (δ) between stress and strain occurs somewhere between the elastic and purely viscous state. The stress signal generated by a viscoelastic material can be separated into two components: an elastic stress (σ') that is in phase with strain, and a viscous stress (σ'') that is in phase with the strain rate and 90° out of phase with the strain. The elastic and viscous stresses are sometimes referred to as the in-phase and out-of-phase stresses, respectively.

Fig. 2 presents several key curves that are often encountered when discussing glass transition temperatures with DMA results, i.e. the evolution of the dynamic or storage modulus E' , the loss modulus E'' , and the loss factor $\tan(\delta) = E''/E'$ (also representative for the material's damping characteristics) with regard to the temperature. A first possibility is to define T_g as the temperature

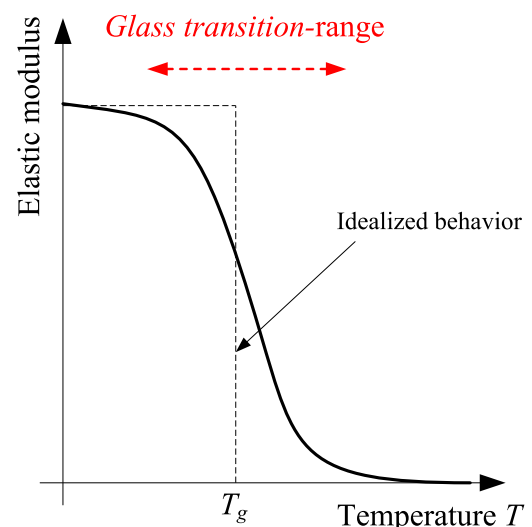


Fig. 1. Schematic elastic modulus loss of an epoxy resin with increasing temperature.

corresponding to the inflection point of the dynamic modulus curve as presented in a). This definition is for instance followed by the ISO 6721-11 [20]. As presented in Fig. 2b, the intersection point between the two tangent lines defines a value for T_{onset} , marking the beginning of the storage modulus loss of the material and considered as the glass transition temperature by ASTM E1640 [21], DIN EN 61006 [22], and DIN 65583 [23]. The latter, mainly used in aerospace industry, also presents an alternative definition by decreasing the initial storage modulus slope by 2% and choosing the intersection with the modulus curve as the representative glass transition temperature. In Fig. 2c the evolution of the viscous (loss) modulus E'' is given. Eventually, in research activities, the loss factor $\tan(\delta)$ (see Fig. 2d) is mainly adopted for the evaluation of T_g [24–30]. Occasionally, the temperature at maximum loss modulus is considered [31].

3. Experimental investigation

3.1. Specimen preparation and curing configurations

Three commercially available products, namely S&P Resin 220 by S&P Clever Reinforcement AG, Sikadur 30 and Sikadur 30 LP by Sika, were used for the present study. All products are two-component pre-batched thixotropic epoxy resins. To the authors' knowledge,

no particular additional fillers are used by the producers. The three products will be described as Resin 1, Resin 2, and Resin 3, respectively, throughout the whole manuscript. Two different curing conditions and ages were taken into account. Table 1 summarizes the glass transition temperature according to the literature [31] or suppliers' data sheets [2,3]. Additional information about physical and mechanical properties are given in Table 2.

For curing purposes, the epoxy was mixed under room temperature conditions and filled in a square mold (shown in Fig. 3). Specimens intended for curing at room temperature were subsequently stored in a climate chamber with a constant temperature of 21°C and a relative humidity of 50%. The remaining specimens designated for accelerated curing were installed under a specifically designed heating device usually used in structural retrofitting applications [14,18,32].

The heating procedure is kept identical to the above mentioned application for the gradient anchorage [14,33], i.e. an epoxy temperature of about 90°C for 25 min, composed of a temperature ramp of about 4–5 min followed by a more or less stable temperature plateau during 20 min. For both room temperature and accelerated curing configurations, a schematic temperature evolution in time is given in Fig. 4. Subsequently, the specimens are also placed in the aforementioned climate chamber at 21°C until testing at either 3 or 28 days. Prior to testing, the cured elements

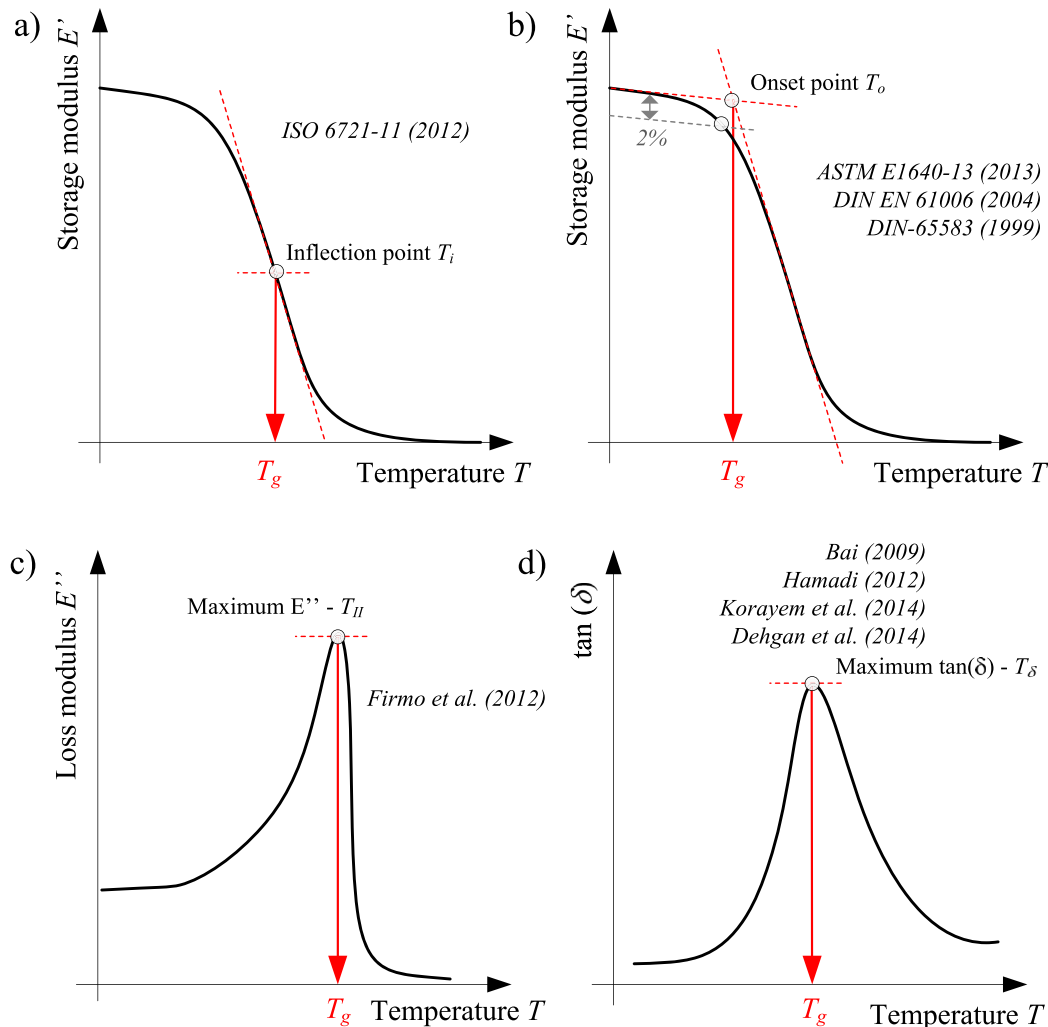


Fig. 2. Schematic representation of several key temperature values during the glass transition.

Table 1
Glass transition temperature T_g according to the literature and suppliers' data sheets.

Epoxy	T_g [°C]
Resin 1: S&P Resin 220	54.5–62.1 (depending on the chosen heating rate during the test) [31]
Resin 2: Sikadur 30	62 (after 7 days at 45°C) [2]
Resin 3: Sikadur 30 LP	45 (after 7 days at 23°C) or 72 (after 2 h at 80°C) [3]

Table 2
Mechanical and physical data according to the suppliers' data sheets [1–3].

	Density [g/cm ³]	Comp. strength [MPa]	E-modulus [MPa]	Pot life [min]
Resin 1	1.7–1.8 at 23°C	>70	>7100	25' at 23°C
Resin 2	1.65 at 23°C	85–95 after 7 days at 35°C	9600 (Compression), 11,200 (Tension), after 14 days cure at 23°C	90 at 20°C, 20 at 35°C
Resin 3	1.8 at 20°C	>85 after 7 days at 25°C	10,000 after 14 days at 25°C	60 at 25°C, 30 at 55°C

were taken out of the mold and cut into small specimens with dimensions of about 45·5·3 mm³.

3.2. Test program

The complete test program with the investigated parameters is presented in the left half of Table 3. The applied temperature profiles during the DMA testing are graphically presented in Fig. 5.

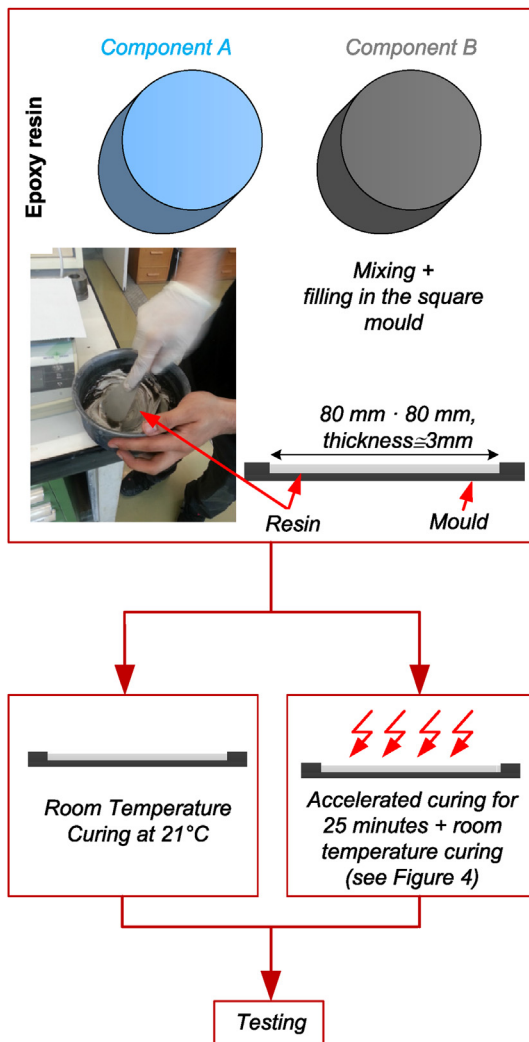


Fig. 3. Procedure for the experimental campaign.

3.3. Test setup

Three-point bending with simple supports as shown in Fig. 6a was chosen as loading configuration. The instrumentation (Type 'RSA III' by TA Instruments) is shown in Fig. 6b. Dynamic mechanical testing involves the application of an oscillatory strain to a specimen over a specific temperature range from a lower (T_{min}) to an upper value T_{max} and back to T_{min} (Fig. 5). Loading frequency was in this case 1 Hz. To run on all temperatures below room temperature, liquid nitrogen was used to cool the inner part of the climate chamber.

4. Results and discussion

The presented evaluation techniques for T_g were applied for all the tested specimens. As an example, Fig. 7 shows the storage modulus, loss modulus, and $\tan(\delta)$ evolution as a function of the applied temperature for Resin 1 after an accelerated curing procedure followed by a room temperature curing for 3 days. All results are summarized in Table 3. Due to both increasing and decreasing branches of the temperature, each test shows two values for each evaluation technique. It has to be stated that for each curing and

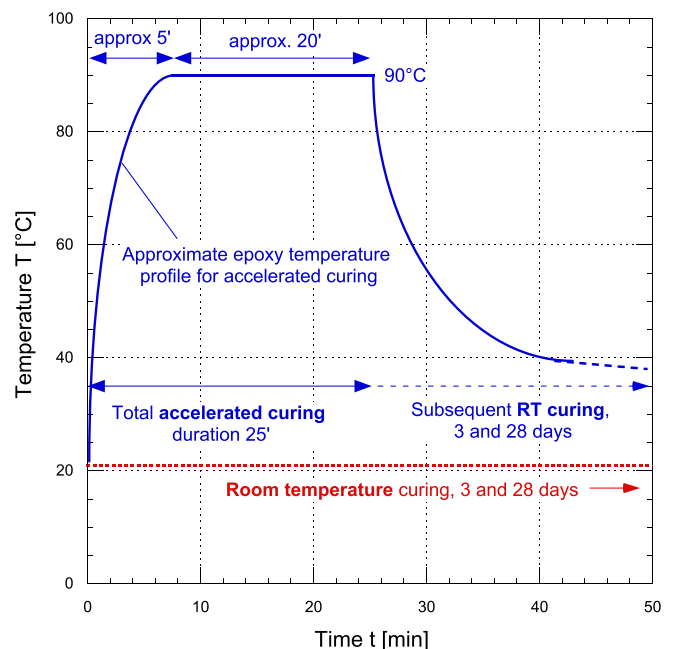


Fig. 4. Curing temperatures for room temperature (RT) and accelerated curing (AC).

Table 3
Varying parameters and summary of all DMA test results with the respective evaluation methods (*upper row: increasing temperature branch, **lower row: decreasing temperature branch) - for notations of T_g see Fig. 2.

	Curing	Age [days]	T_{min} [°C]	T_{max} [°C]	Rate [°C/min]	T_{δ} [°C]	T_i [°C]	T_o [°C]	T_{II} [°C]
Resin 1	RT	3	-20	100	2	*53.1	46.6	42.8	45.7
						**72.7	58.0	50.7	56.0
Resin 1	RT	3	-20	150	2	55.1	46.6	42.4	46.8
						78.5	65.0	50.3	65.8
Resin 1	AC	3	-20	100	2	64.8	52.3	37.2	51.8
						71.6	59.3	43.8	61.8
Resin 1	RT	28	-20	100	2	67.9	56.6	43.6	56.5
						75.4	60.2	49.4	64.0
Resin 2	RT	3	-20	100	2	51.3	45.7	43.8	46.5
						68.7	59.6	49.2	59.2
Resin 2	RT	3	-20	100	0.5	56.0	42.3	41.2	46.2
						73.2	65.4	53.1	64.5
Resin 2	AC	3	-20	100	2	62.6	52.8	44.4	54.4
						70.3	61.6	52.8	62.4
Resin 2	RT	28	-20	100	2	54.7	48.3	46.5	49.4
						69.8	60.7	49.7	61.0
Resin 3	RT	3	-20	100	2	59.2	47.5	45.1	49.1
						84.9	75.0	61.3	75.6
Resin 3	AC	3	-20	100	2	73.5	57.6	45.7	58.9
						88.9	79.4	67.7	79.6

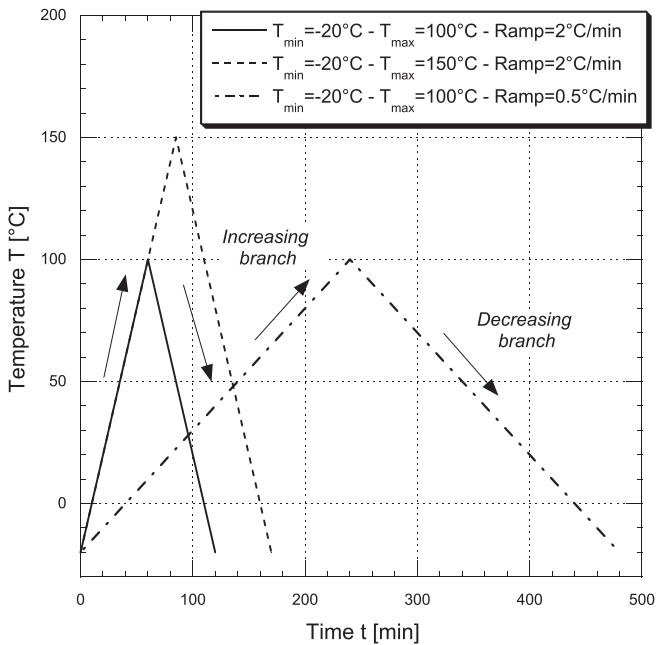


Fig. 5. Temperature profiles during DMA testing.

testing condition, only one specimen has been tested. Variability of the results was in this case not considered.

4.1. Influence of the evaluation method and temperature history

A first very important observation from Table 3 is the fact that different evaluation methods result in large differences in the results. These large discrepancies are of very high importance when talking about a glass transition temperature in general. In Section 2.2, it was reported that different testing recommendations sometimes use different definitions for the glass transition temperature. The general tendency for all the tested specimens is that the highest values are obtained when choosing T_{δ} as the evaluation temperature for T_g . In such a case, a difference of more than 10°C to for instance the values for T_i and T_{II} can be observed. The most conservative approach is choosing the onset point T_o at the tangent intersection. This first observation confirms that every statement about a specific value for T_g should always include precisions about the chosen evaluation method, which in most cases is not indicated by the producer or distributor.

The second information obtained is that the decreasing branch of the temperature exhibits higher values for the glass transition temperature T_g than the first increasing branch. In Figs. 8–11 as well as in Table 3, this effect is confirmed for all the performed test specimens under the influence of various parameters. This is due to an improved cross-linking of the polymer chains after the first heating step of the DMA analysis. Similar observations with DSC-

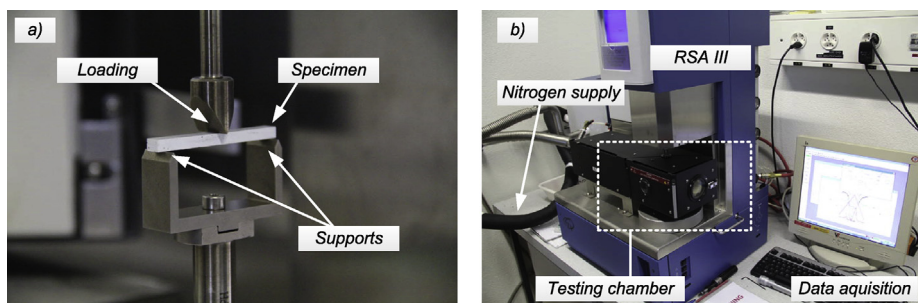
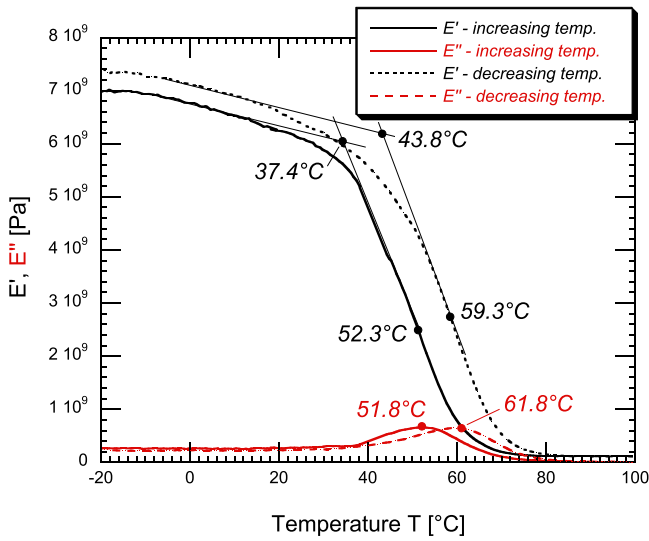
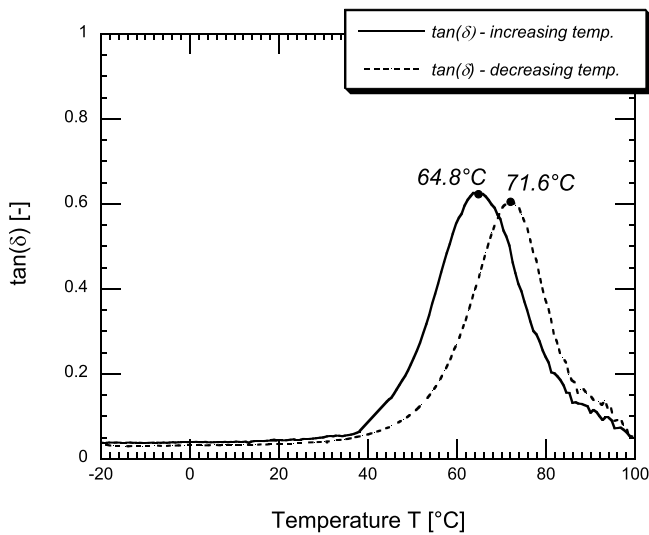


Fig. 6. a) Three-point bending setup, b) RSA III dynamic testing instrumentation.



(a) Storage and loss modulus (E' , E'')



(b) $\tan(\delta)$

Fig. 7. Experimental results for Resin 1 after an initial accelerated curing (AC) followed by a 3 days curing at room temperature.

based tests have been shown by Moussa et al. [34]. In terms of practical applications in structural engineering, this implies that an epoxy resin cured at outer temperature on a construction site might see its temperature characteristics change towards higher glass transition temperatures if one applies post-curing [35]. Nevertheless, this improvement requires an unstressed and unloaded externally bonded CFRP reinforcement, as otherwise load carrying capacity of the strengthened structure might be lost due to a temporary stiffness reduction of the resin during post-curing as a consequence of a decreased storage modulus.

It is also important to remember that a certain human factor might influence the evaluation, especially when it comes to introducing tangent lines into a modulus–time graph. In order to avoid strong influences at this level, the same user should be in charge of evaluating all the data sets later for comparison purposes.

In the following subsections, the $\tan(\delta)$ -evaluation is retained for all other parameter investigation. An overloading of the diagrams is consequently avoided. Using this evaluation puts the

manuscript in line with the large majority of scientific research activities. From Table 3, the effect of the different testing and curing parameters is observed for the different evaluating techniques for T_g . Hence, the approach with choosing one fixed evaluation method for the following parameter analysis seems justified.

4.2. Influence of the product type and curing procedure

Fig. 8 shows a comparison between Resin 1, 2, and 3 for different curing conditions. All specimens were 3 days old at the moment of testing. A first observation is the fact that Resin 3 exhibits a higher glass transition temperature after a normal curing procedure at room temperature. An accelerated curing procedure results for all three types in a relative increase of about 20% in T_g , eventually displaying the highest value of 73.5°C for Resin 3. This increase after an accelerated curing at high temperature is a direct consequence of a stronger chain cross-linking. Secondly, the glass transition temperatures on the decreasing branch are very similar for both RT and AC curing procedures in case of Resin 1 and 2. Resin 3 again exhibits higher values for T_g . Lastly, it can also be observed that for all three resin types, the difference between the glass transition temperature on the increasing and decreasing temperature phase for one curing configuration is still present, nevertheless the relative differences between both stages decreases when an initial accelerated curing phase is introduced ($\Delta T_1 > \Delta T_2$, see Fig. 8).

4.3. Influence of the maximum temperature during testing

Two different temperature peaks of 100 and 150°C (Fig. 5) are considered in Fig. 9. It can be seen that during the increasing temperature branch, both obtained results of 53.1 and 55.1°C are almost identical. In case the test was run up to 150°C, the resulting glass transition temperature also increased by about 8%. All other methods show the same tendency as for the $\tan(\delta)$ -method, as shown in Table 3. This increase in T_g with higher exposure temperature is in accordance with the observations made by Moussa et al. [34].

4.4. Influence of the specimen age

Two tests performed on Resin 1 after 3 and 28 days, respectively, are presented in Fig. 10. Glass transition temperature T_g visibly increases with growing age, being shifted from 53.1 to 67.9°C. The subsequent heating of the specimen above its glass transition range implicates in both cases an increased value for T_g on the decreasing ramp. The relative difference between the increasing and decreasing temperature branch becomes smaller with growing age. Similar results presenting in increase of T_g in time were presented by Moussa et al. [36], in which specimens cured under laboratory conditions for several years were investigated. Another continuous rise in the glass transition temperature over the years was also observed by Chatterjee and Gillespie [37].

4.5. Influence of the heating rate

A last comparison is performed by analyzing the influence of the heating rate, i.e. the rate at which the temperature is increased during the DMA test (Fig. 5). In Fig. 11, it becomes obvious that a slower temperature increase at 0.5°C/min results in slightly higher glass transition values than for a faster rate at 2°C/min. The difference between both is however small with a value below 10%. The observation is indeed contrary to information available in the literature [38–39]. However, both references cover a larger range of heating rates, which are also mostly higher than the ones used in

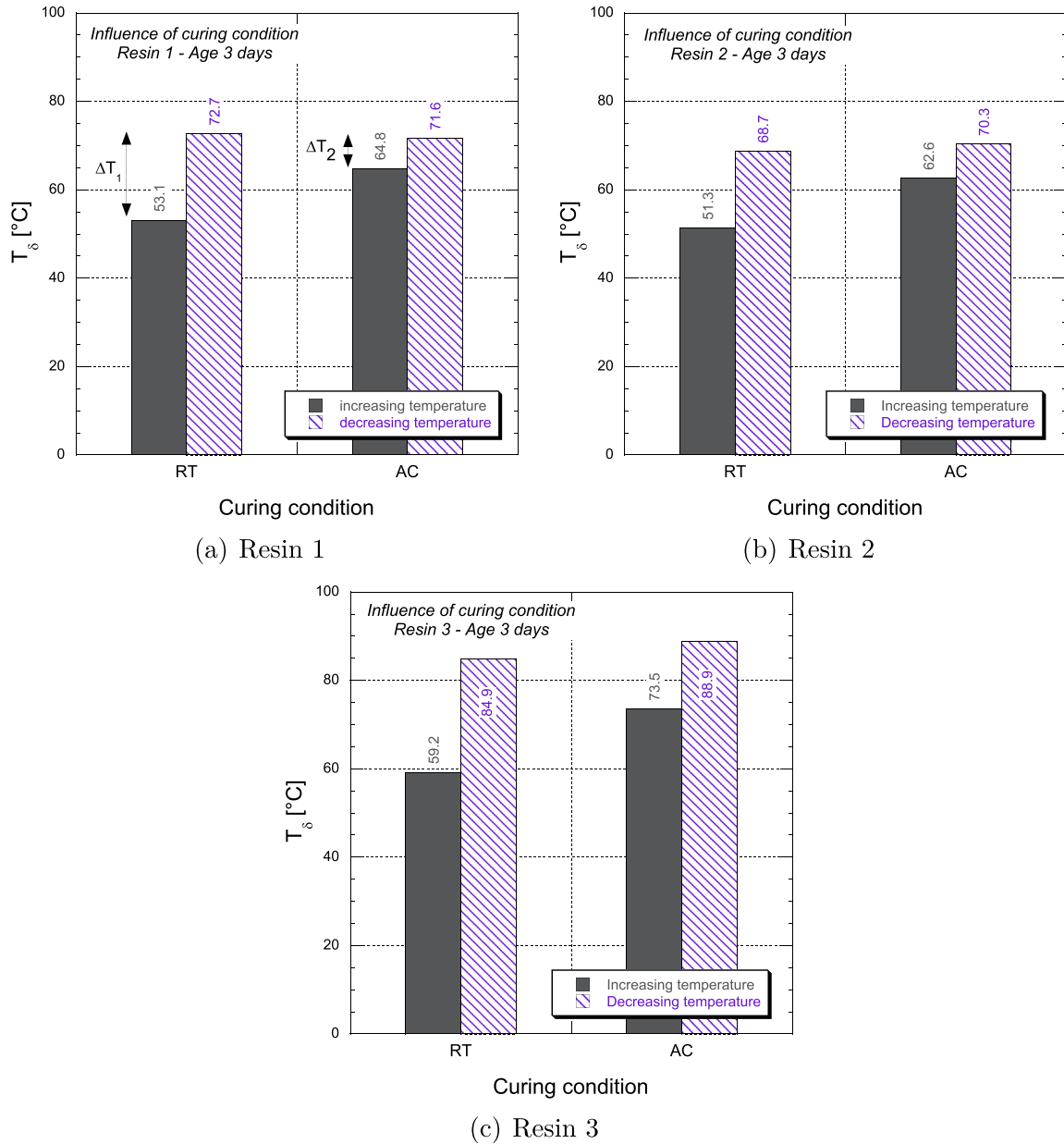


Fig. 8. Influence of the curing procedure for three different epoxy resin types.

this paper. In order to obtain more sound information on the behavior of the investigated resins, additional tests at several different heating rates have to be performed.

5. Service temperatures in civil engineering

For a structural designer, it is of utmost importance to define a maximum service temperature a FRP-retrofitted structure can be exposed to. In several design codes dealing with strengthening existing (concrete) structures, limit temperatures are defined for the epoxy resin in order to avoid stiffness degradation. Usually the allowable service temperature is based on the glass transition temperature of the used epoxy. The former section shows the differences between the assessment of the glass transition temperature itself with regard to testing recommendations. This section discusses the differences in the structural design guidelines defining the allowed service temperature. Table 4 summarizes

several design guidelines with their respective testing method and recommendation as well as their definition of the maximum allowable temperature under service.

In the *fib*-Bulletin 14 [40] published in 2001, it was described that T_g for an applied epoxy should be equal or larger than 45°C or maximum shade air temperature in service has to be lower than $T_g - 20^\circ\text{C}$. As testing method, DSC based on EN 12614 [41] is indicated. The British TR 55 [42] suggests the same testing recommendation when using DSC, but gives an additional testing code for DMA [20]. The maximum allowed service temperature is obtained by subtracting 15°C to the previously determined value of T_g . The guideline also discusses, similar to Stratford and Bisby [43], the effect of using different definitions for the T_g on the final result. Clear indications in terms of testing are also given by the Italian CNR-DT 200 R1/2013 [44], the maximum allowed service temperature, in case no special insulation is used, is also limited to $T_g - 15^\circ\text{C}$. The same limitation is again given by the American ACI

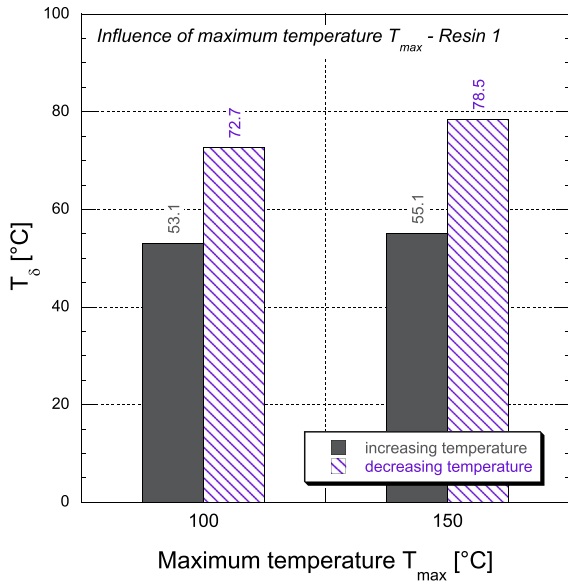


Fig. 9. Influence of the maximum heating temperature.

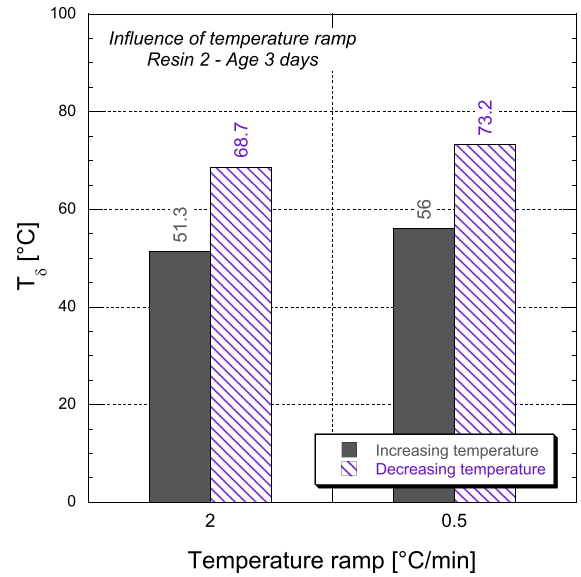


Fig. 11. Influence of the temperature heating rate [°C/min].

440 [45]. Several other design codes are however much less precise in their indications: Swiss SIA 166 [46], Canadian ISIS [47], and Australian HB 305 [48] do not list precise information neither on how to obtain the glass transition temperature nor on how to consider environmental temperature. The structural designer is listed as responsible person to define limits according to the product's characteristics. The DAfStb-Richtlinie [49] refers to the usually applied national approvals.

Ferrier et al. [10], based on creep investigations, stated that T_g should be higher than 55°C, or otherwise the service temperature should be limited to $T_g - 15^\circ\text{C}$ in case of lower glass transition temperatures. Klamer [50] showed that the previously defined margin of -20°C as defined by the fib-Bulletin 14 [40] can be reduced to -10°C .

The listed explanations clearly show that obvious differences between national design guidelines for structural strengthening

with composite materials exist. For instance, both the American ACI 440 [45] as well as the British TR 55 [42] limit the maximum service temperature to the value of $T_g - 15^\circ\text{C}$. However, according to the respective testing recommendations, either the value of the onset temperature T_o (ACI 440) or the inflection point T_i (TR 55) has to be considered for evaluating T_g . From Table 3, it becomes obvious that for one product differences of more than 10 °C can arise depending on the chosen design code. The obtained values for instance for T_o and T_i are located between approximately 40 and 55°C, in most cases however below 50°C.

In 2013, temperature measurements under a 4 cm-asphalt layer on a pedestrian bridge in Rümlang (Switzerland) have been performed in the framework of a research project at Empa. The outer temperature was at that moment about 33°C and the asphalt layer was directly exposed to the sun. At the time of measuring, temperatures under the mentioned asphalt layer were about 55°C, a value that can also be assumed for the epoxy resin in case a strengthening would be located at this place. Compared to the previously mentioned values, structural integrity with commercially available resins would not be assured according to several of the described guidelines.

6. Conclusions & recommendations

The presented investigations have shown that the glass transition temperature is not a defined material property, but it depends on several curing and testing parameters. This is critical since it is used for the definition of a maximum service temperature for civil structures. Several conclusions can be drawn:

- The measured glass transition temperatures of three commercial epoxies used in structural strengthening without post-curing for structural applications showed rather low values in the region of 40–50°C, which are in the range of service temperatures that might occur in civil structures.
- Generally all tests confirm the expected behavior that the glass transition temperature increases after an accelerated procedure as a result of a higher cross-linking of the polymer chains.
- Glass transition temperature rises with the epoxy's age. Hence, laboratory testing should, if possible, accommodate this circumstance. A too conservative approach by testing specimens

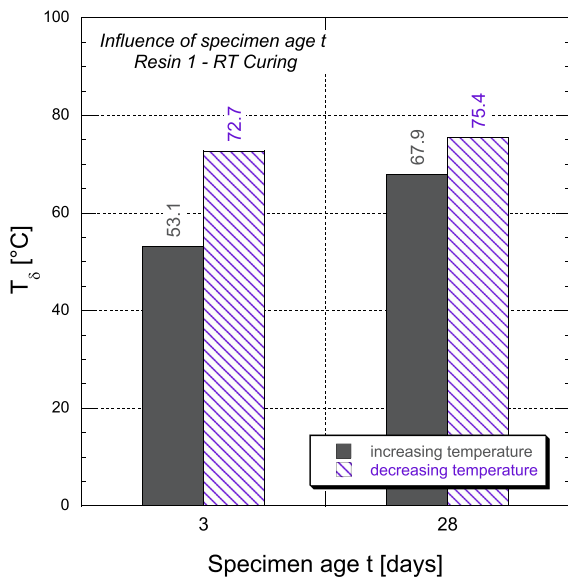


Fig. 10. Influence of the specimen age.

Table 4Structural design guidelines with corresponding testing recommendations for the assessment of T_g and definition of allowed temperature under service.

Guideline	Reference for testing	Service temperatures
fib bulletin 14 [40] TR 55 [42]	DSC: EN 1504-4 [51], EN 12614 [41] DSC: EN 1504-4 [51], EN 12614 [41] DMA: ISO 6721 [20]	$T_g \geq 45^\circ\text{C}$ or maximum shade temperature $\leq T_g - 20^\circ\text{C}$ $T_g - 15^\circ\text{C}$
DAfStb Guideline [49] SIA 166 [46]	None - Reference to the national product certifications None	Service limits depending on T_g defined in the national approvals Maximum service temperature to be declared by the supplier according to the resin's thermomechanical properties $T_g - 15^\circ\text{C}$, otherwise special insulation is required
CNR [44] ACI 440 [45] ISIS Canada [47]	DSC: ISO 11357-2 [52], ASTM E1356 [53] DMA: ISO 11359-2 [54], ASTM E1640 [21] DMA: ASTM E1640 [21] None	$T_g - 15^\circ\text{C}$ for dry environments, in other situations special testing is required Maximum service temperature to be declared by the engineer based on the resin's thermomechanical properties provided by the supplier Engineer should consider glass transition in the design
HB 305 [48]	None	

at a too young age compared to a later usage in practice would be wrong from both an engineering and economic point of view. A specimen age of 28 days could be reasonable for testing when service temperature is the relevant factor. In case other temperature scenarios (for instance mastic asphalt application) have to be considered, the age of the testing specimens should be as close as possible to the epoxy's age installed on site at the relevant date.

- The curing procedure as well as the maximum temperature during the DMA testing was also revealed to be important. The designer should verify whether a post-curing of the epoxy resin is possible. If so, significantly higher values for the glass transition can be obtained. It is believed that post-curing allows for more structural safety due to initially lower values of T_g for only cold-curing adhesives.
- Since the heating rate also plays a role in the final results, one should try to obtain as much information as possible about the real temperature scenario that might occur on the structure and how fast the respective situations can appear. This can help to define an adequate temperature increase in time for the specimen testing and thus obtain meaningful results.
- Large differences in values depending on the evaluation technique ($\tan(\delta)$, maximum slope of the storage modulus, etc.) are obvious. The indication of a glass transition temperature in a technical data sheet for a certain adhesive should therefore always be complemented with information about the chosen test parameters and evaluation method. It is further important for the structural designer to judge the suitability of an adhesive for a specific application.
- Considering the knowledge of the glass transition of an epoxy, the structural designer has to evaluate its suitability for a specific strengthening application considering the structure's temperature exposure.
- In future, guidelines should be unified in order to clarify the procedure on how to determine T_g and how to set it in relation with the outer service exposure temperature.

Acknowledgments

Acknowledgments are addressed to Max Heusser from the Structural Engineering Research Laboratory (Empa) for the help with the specimen preparation, as well as both industrial partners S&P Clever Reinforcement AG (Switzerland) and Sika (Switzerland) for their material contribution. The financial contribution of the Swiss Road Authorities (FEDRO/ASTRA) within the framework of the project AGB 2012/001 is also appreciated.

References

- [1] S&P-Clever-Reinforcement-Company-AG. S&P resin 220 epoxy adhesive - technical data sheet. S&P Clever Reinforcement Company AG; 2013. Available from: www.reinforcement.ch.
- [2] Sika. Sikadur-30 adhesive for bonding reinforcement - product data sheet. Sika; 2006.
- [3] Sika. Sikadur-30 LP adhesive for bonding reinforcement - product data sheet. Sika; 2006.
- [4] Meier U. Strengthening of structures using carbon fibre/epoxy composites. *Constr Build Mater* 1995;9(6):341–51.
- [5] Bakis CE, Bank LC, Brown VL, Cosenza E, Davalos JF, Lesko JJ, et al. Fiber-reinforced polymer composites for construction - state-of-the-art review. *J Compos Constr* 2002;6(2):73–87.
- [6] Zoghi M, editor. The international handbook of FRP composites in civil engineering. CRC Press; 2014.
- [7] Moussa O, Vassilopoulos AP, Keller T. Effects of low-temperature curing on physical behavior of cold-curing epoxy adhesives in bridge construction. *Int J Adhesion Adhesives* 2012;32(1):15–22.
- [8] Leone M, Matthys S, Aiello MA. Effect of elevated service temperature on bond between FRP EBR systems and concrete. *Compos Part B* 2009;40:85–93.
- [9] Zilch K, Zehetmaier K, Borchert K, Endres B, Fischer O. Die Rösllautalbrücke bei Schirding - Innovative Verfahren zur Verstärkung einer Spannbetonbrücke (in German). *Bauingenieur* 2004;79:589–95.
- [10] Ferrier E, Michel L, Jurkiewicz B, Hamelin P. Creep behavior of adhesives used for external FRP strengthening of RC structures. *Constr Build Mater* 2011;25:461–7.
- [11] Chataigner S, Caron J-F, Benzarti K, Quiertant M, Aubagnac C. Use of a single lap shear test to characterize composite-to-concrete or composite-to-steel bonded interfaces. *Constr Build Mater* 2011;25(2):468–78.
- [12] Houhou N, Benzarti K, Quiertant M, Chataigner S, Fléty A, Marty C. Analysis of the nonlinear creep behavior of concrete/FRP-bonded assemblies. *J Adhes Sci Technol* 2014;28(14–15):1345–66.
- [13] Silva P, Fernandes P, Sena Cruz J, Azenha M, Barros J. Creep behavior and durability of concrete elements strengthened with NSM CFRP strips. In: CICE 2014. Vancouver, Canada; 2014.
- [14] Michels J, Sena Cruz J, Czaderski C, Motavalli M. Structural strengthening with prestressed CFRP strips anchored with the gradient method. *J Compos Constr (ASCE)* 2013;17(5):651–61.
- [15] Czaderski C, Martinelli E, Michels J, Motavalli M. Effect of curing conditions on strength development in an epoxy resin for structural strengthening. *Compos Part B: Eng* 2012;43(2):398–410.
- [16] Moussa O, Vassilopoulos AP, de Castro J, Keller T. Early-age tensile properties of structural epoxy adhesives subjected to low-temperature curing. *Int J Adhes Adhes* 2012;35:9–16.
- [17] Kotynia R, Walendziak R, Stöcklin I, Meier U. RC slabs strengthened with prestressed and gradually anchored CFRP strips under monotonic and cyclic loading. *J Compos Constr (ASCE)* 2011;15(2):168–80.
- [18] Michels J, Martinelli E, Czaderski C, Motavalli M. Prestressed CFRP strips with gradient anchorage for structural concrete retrofitting: experiments and numerical modeling. *Polymers* 2014;6(1):114–31.
- [19] Hülder G, Dallner C, Ehrenstein GW. Curing of epoxy-adhesives for the supplementary reinforcement of buildings with bonded CFRP-straps (in German). *Bauingenieur* 2006;81:449–54.
- [20] ISO-6721-11. Plastics - determination of dynamic mechanical properties - part 11: glass transition temperature. ISO International Standard; 2012.
- [21] ASTM-E1640-13. Standard test method for the glass transition temperature by dynamic mechanical analysis. ASTM International; 2013.
- [22] DIN-EN-61006. Electrical insulating materials - methods of test for the determination of the glass transition temperature. Deutsches Institut für Normung; 2004.

- [23] DIN-65583. Faserverstärkte Kunststoffe - Bestimmung des Glasübergangs von Faserverbundwerkstoffen unter dynamischer Belastung. Deutsches Institut für Normung; 1999.
- [24] Korayem AH, Barati MR, Simon GP, Zhao XL, Duan WH. Reinforcing brittle and ductile epoxy matrices using carbon nanotubes masterbatch. *Compos Part A: Appl Sci Manuf* 2014;61:126–33.
- [25] Hamadi Z. Etude du comportement d'un composite verre/polyester sous sollicitations thermiques. Mémoire de Magister. Boumerdes: Université M'Hamed Bougara; 2012.
- [26] Bai Y. Material and structural performance of fiber-reinforced polymer composites at elevated and high temperatures [PhD Thesis]. Ecole Polytechnique Fédérale de Lausanne (EPFL); 2009. p. 332.
- [27] Dehgan M, Al-Mahaidi R, Sbarski R, Gad E. Effect of fabrication method of thermo-mechanical properties of an epoxy composite. *J Adhes* 2014;90(5–6): 368–83.
- [28] Nguyen TMH. Caractérisation du vieillissement d'une peinture acrylique en phase aqueuse. Rapport de stage. Université de Toulon et du Var; 2002.
- [29] Gojny FH, Schulte K. Functionalization effect on the thermo-mechanical behaviour of multi-wall carbon nanotube/epoxy-composites. *Compos Sci Technol* 2004;64:2303–8.
- [30] Xian G, Karbhari VM. Segmental relaxation of water-aged ambient cured epoxy. *Polym Degrad Stab* 2007;92:1650–9.
- [31] Firmo JP, Correia JR, França P. Fire behavior of reinforced concrete beams strengthened with CFRP laminates: protection systems with insulation of the anchorage zones. *Compos Part B: Eng* 2012;43:1545–56.
- [32] Michels J, Czaderski C, El-Hacha R, Brönnimann R, Motavalli M. Temporary bond strength of partly cured epoxy adhesive for anchoring prestressed CFRP strips on concrete. *Compos Struct* 2012;94(9):2667–76.
- [33] Michels J, Zile E, Czaderski C, Motavalli M. Debonding failure mechanisms in prestressed CFRP/epoxy/concrete connections. *Eng Fract Mech* 2014;132: 16–37.
- [34] Moussa O, Vassilopoulos AP, de Castro J, Keller T. Time-temperature dependence of thermomechanical recovery of cold-curing structural adhesives. *Int J Adhes Adhes* 2012;35:94–101.
- [35] Sika. Sika CarboHeater. Sika; 2001. Available from: www.sika.com.
- [36] Moussa O, Vassilopoulos AP, Castro JD, Keller T. Long-term development of thermophysical and mechanical properties of cold-curing structural adhesives due to post-curing. *J Appl Polym Sci* 2013;127(4):2490–6.
- [37] Chatterjee A, Gillespie Jr JW. Room temperature-curable VARTM epoxy resins: promising alternative to vinyl ester resins. *J Appl Polym Sci* 2010;115(2): 665–73.
- [38] Jankowsky JL, Wong DG, DiBerardino MF, Cochran RC. Evaluation of upper use temperature of toughened epoxy adhesives. In: Assignment of the glass transition, ASTM STP 1294; 1994.
- [39] Sun W, Vassilopoulos AP, Keller T. Effect of thermal lag on glass transition temperature of polymers measured by DMA. *Int J Adhes Adhes* 2014;52:31–9.
- [40] fib Bulletin 14. Externally bonded FRP reinforcement for RC structures. fib, International federation for structural concrete; 2001. p. 130.
- [41] DIN-EN-12614. Products and systems for protection and repair of concrete structures - test methods - determination of glass transition temperature. Deutsches Institut für Normung; 2005.
- [42] TR55. Design guidance for strengthening concrete structures using fibre composite materials. The Concrete Society (UK); 2012. p. 187.
- [43] Stratford TJ, Bisby LA. Effect of warm temperatures on externally bonded FRP strengthening. *J Compos Constr (ASCE)* 2012;16(3):235–44.
- [44] CNR. Istruzioni per la Progettazione, l'Esecuzione ed il Controllo di Interventi di Consolidamento Statico mediante l'utilizzo di Compositi Fibrorinforzati. In: Consiglio nazionale delle ricerche (National Research Council) - Commissione di studio per la predisposizione e l'analisi (Italy); 2013. p. 144.
- [45] ACI440.2R. Guide for the design and construction of externally bonded FRP systems for strengthening concrete structures. American Concrete Institute; 2008. p. 80.
- [46] SIA166. Klebebewehrungen. Switzerland: SIA - Schweizer Ingenieur- und Architektenverein; 2004. p. 44.
- [47] ISIS. Strengthening reinforced Concrete structures with externally-bonded fibre reinforced polymers. The Canadian Network of Centres of Excellence on Intelligent Sensing for Innovative Structures (Canada). 2007.
- [48] HB305. Design handbook for RC structures retrofitted with FRP and metal plates: beams and slabs. Standards Australia. 2008. p. 80.
- [49] DAfStb. Guideline - strengthening of concrete members with adhesively bonded reinforcement. Deutscher Ausschuss für Stahlbeton (DAfStb, Germany); 2012.
- [50] Klamer E-L. Influence of temperature on concrete beams strengthened in flexure with CFRP [PhD thesis]. TU Eindhoven; 2009.
- [51] DIN-EN-1504-4. Products and systems for the protection and repair of concrete structures - definitions, requirements, quality control and evaluation of conformity - part 4: structural bonding (German version). Deutsches Institut für Normung; 2005. p. 121.
- [52] ISO-11357-2. Plastics - differential scanning calorimetry (DSC) - part 2: determination of glass transition temperature. ISO International Standard; 1999.
- [53] ASTM-E1356-08. Standard test method for assignment of the glass transition temperatures by differential scanning calorimetry. ASTM International; 2014.
- [54] ISO-11359-2. Plastics - thermomechanical analysis (TMA) - part 2: determination of coefficient of linear thermal expansion and glass transition temperature. ISO International Standard; 1999.